

Communication: Phase incremented echo train acquisition in NMR spectroscopy

Jay H. Baltisberger,¹ Brennan J. Walder,² Eric G. Keeler,² Derrick C. Kaseman,² Kevin J. Sanders,² and Philip J. Grandinetti^{2,a)}

¹*Division of Natural Science, Mathematics, and Nursing, Berea College, Berea, Kentucky 40403, USA*

²*Department of Chemistry, Ohio State University, 100 West 18th Avenue, Columbus, Ohio 43210, USA*

(Received 1 May 2012; accepted 24 May 2012; published online 4 June 2012)

We present an improved and general approach for implementing echo train acquisition (ETA) in magnetic resonance spectroscopy, particularly where the conventional approach of Carr-Purcell-Meiboom-Gill (CPMG) acquisition would produce numerous artifacts. Generally, adding ETA to any N -dimensional experiment creates an $N + 1$ dimensional experiment, with an additional dimension associated with the echo count, n , or an evolution time that is an integer multiple of the spacing between echo maxima. Here we present a modified approach, called phase incremented echo train acquisition (PIETA), where the phase of the mixing pulse and every other refocusing pulse, ϕ_P , is incremented as a single variable, creating an additional phase dimension in what becomes an $N + 2$ dimensional experiment. A Fourier transform with respect to the PIETA phase, ϕ_P , converts the ϕ_P dimension into a Δp dimension where desired signals can be easily separated from undesired coherence transfer pathway signals, thereby avoiding cumbersome or intractable phase cycling schemes where the receiver phase must follow a master equation. This simple modification eliminates numerous artifacts present in NMR experiments employing CPMG acquisition and allows “single-scan” measurements of transverse relaxation and J -couplings. Additionally, unlike CPMG, we show how PIETA can be appended to experiments with phase modulated signals after the mixing pulse.

© 2012 American Institute of Physics. [<http://dx.doi.org/10.1063/1.4728105>]

Echo train acquisition (ETA) is a powerful approach in magnetic resonance, forming the basis of a number of diverse and advanced magnetic techniques such as echo planar imaging¹ in MRI, diffusion and transverse relaxation measurements,^{2–6} ultra-fast multi-dimensional liquid state NMR,⁷ and sensitivity enhancement in solid-state NMR.⁸ The primary benefits of ETA are reduced experiment time, enhanced sensitivity, and the ability to separate frequency contributions that are refocused during the echo train pulse sequence from those that are not. Here we present an improved method, called phase incremented echo train acquisition (PIETA), for adding ETA to a number of NMR experiments where the standard approach of Carr-Purcell-Meiboom-Gill (CPMG) acquisition would produce numerous artifacts.

In CPMG acquisition, shown in Fig. 1(a), a train of rf pulses produces a train of echo signals arising from the refocusing of frequency contributions with odd symmetry in their spin transition function.⁹ Frequency contributions lacking odd symmetry result in a modulation or decay of the echo train signal. In principle, the echo amplitude modulations in liquid-state CPMG experiments could be used to measure unfocused J -coupling frequency contributions when the size of the couplings is smaller than the linewidth from magnetic field inhomogeneities.¹⁰ Additionally, the echo amplitude decays in CPMG could be related to transverse relaxation rates independent of molecular diffusion rates.^{2,3} It is well

known,^{4,5,11–14} however, that CPMG acquisition can often fail to produce desired results because non-ideal rf pulses introduce contaminating signals from undesired coherence transfer pathways.

Ideally, each echo observed in a CPMG experiment is the result of a coherence transfer from $p = +1 \rightarrow -1$ by a single rf pulse. If the rf pulse creating the transfer is a perfect π rotation of the magnetization, then the efficiency of this transfer is 100%. Unfortunately, resonance offset effects, as well as rf field inhomogeneities, lead to inefficient transfers. Thus, coherences may “leak” into undesired pathways, i.e., $p = +1 \rightarrow 0$ and $p = +1 \rightarrow +1$. In ETA even the smallest inefficiencies lead to significant signal loss since the intensity of the echo after n transfers is reduced by the transfer efficiency to the n th power. While these intensity losses are real, they are generally unobservable because they are “buried” under undesired echo signals coming from various stimulated echoes, that is, the undesired pathways. This effect leads to multi-exponential CPMG echo decays in situations where perfect π pulses would yield only a single exponential.⁴ Additionally, any attempts to measure J -couplings from the modulation of the CPMG echo train amplitude become intractable because of signal contamination from undesired pathways.

Clearly, a challenge in using ETA acquisition is in obtaining perfect refocusing and eliminating undesired signal pathways. In CPMG, one can strive for perfect π pulses through higher rf powers and restricting the sample to the most homogeneous part of the rf transmitter coil, but these approaches have drawbacks. For example, smaller rf coils can provide a

^{a)}URL: <http://www.grandinetti.org>.

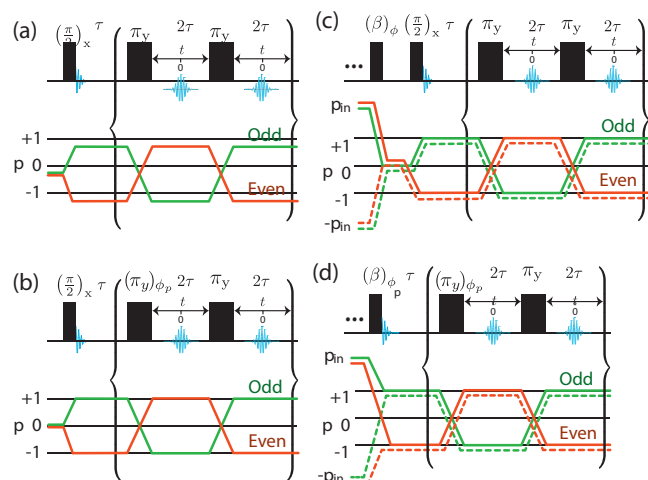


FIG. 1. (a) The original CPMG acquisition sequence.³ (b) The PIETA sequence that replaces the CPMG sequence in (a). (c) CPMG acquisition appended to a sequence with a phase modulated coherence of order p_{in} prior to being converted into observable coherence of $p = -1$. With CPMG acquisition, the input coherence must pass through a $p = 0$ level (z -filter) and be converted into amplitude modulated signal before acquisition. (d) PIETA is appended to a sequence with a phase modulated coherence of order p_{in} prior to mixing down for acquisition. Because PIETA does not have the z -filter requirement, it can separate degenerate pathways where CPMG acquisition cannot, and additionally gains a $\sqrt{2}$ improvement in sensitivity over CPMG acquisition.

higher rf field strength but at the price of smaller sample volume which, coupled with sample restriction, can be severely limiting for sensitivity. While perfect refocusing pulses in CPMG are the panacea to the problems described above, a significant subset of these problems can be solved by simply eliminating the undesired coherence transfer pathways. The most obvious solution, proposed decades ago by Bain¹⁵ and Bodenhausen *et al.*,¹⁶ would be to cycle the pulse and receiver phases during signal coaddition according to a master equation to eliminate the undesired coherence transfer pathways. This approach, however, cannot be easily applied to CPMG acquisition because the phase cycle for n refocusing pulses is, at minimum, on the order of 2^n steps. Thus, no pulse sequence using CPMG acquisition, even with “cogwheel” phase cycling,¹⁷ has been published that eliminates these artifacts. Since every observed echo can have contributions from multiple pathways, the challenge is to find a master equation for the receiver phase as a function of echo count that dealias (unfolds) all desired pathway signals away from undesired pathway signals.

Here we present a simple solution, based on the seminal work of Drobny *et al.*,¹⁸ which exploits the signal as a function of ϕ_p , the pulse phase, being the Fourier conjugate of the signal as a function of Δp , the coherence order change during the pulse.¹⁹ Generally, in ETA, an N -dimensional experiment becomes an $N + 1$ dimensional experiment, with an additional dimension associated with the echo count, n , or an evolution time that is an integer multiple of the spacing between echo maxima. In PIETA, the mixing pulse and every other refocusing pulse are incremented by a phase, $\Delta\phi_p$, creating an $N + 2$ dimensional experiment with the additional phase dimension. A Fourier transform with respect to the PIETA phase, ϕ_p ,

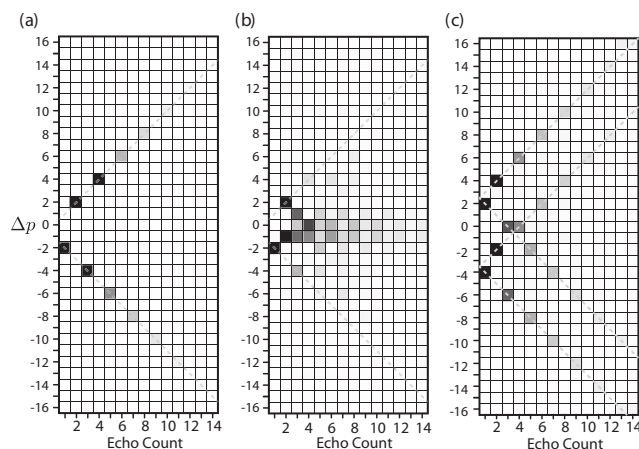


FIG. 2. Experimental 2D PIETA cross sections taken through the time origin. (a) A magic-angle spinning (MAS)-PIETA cross section of RbNO_3 using the sequence in Fig. 1(b), where the π pulse width has been calibrated and no undesired pathway signals are observed. The Δp range from -16 to $+16$ was obtained using $\Delta\phi_p = 2\pi/32$. The cross section in (b) was obtained with the same sequence and sample as (a) except the refocusing pulse was intentionally mis-set to $\pi/2$ to illustrate the presence of undesired pathway signals. (c) Experimental 2D cross section taken through the echo maximum at $t_1 = 0$ and $t_2 = 0$ in a 4D Multiple-quantum MAS (MQMAS)-PIETA spectrum of RbNO_3 using $\Delta\phi_p = 2\pi/32$.

converts the ϕ_p dimension into a Δp dimension. The simplest application of PIETA, shown in Fig. 1(b), is after a $\pi/2$ excitation pulse, which leads to a 3D signal, $S(t, n, \Delta p)$. Shown in Fig. 2(a) is the experimental 2D cross section at $t = 0$ for such a signal in the case of the ^{87}Rb MAS NMR signal of polycrystalline RbNO_3 . As can be seen in Fig. 2(a), the PIETA cross section with the Δp and n dimensions contains a “V” pattern of intensity from the desired pathways. The signals in the “squares” belonging to the desired pathways are extracted into a 2D signal as a function of t and n . If there is no frequency modulation along the n dimension, then one might further reduce the signal in a weighted average to maximize sensitivity²⁰ into a 1D signal as a function of t . In Fig. 2(b), the refocusing pulse was intentionally mis-set to $\pi/2$ to make more prominent the undesired pathway signals, which appear inside the pattern of the desired pathway signals. The undesired pathway signals arise from stimulated echoes, and decay at a slower rate than the desired pathway signal.

Another important advantage of PIETA is that it can be appended to experiments with a phase modulated signal after the mixing pulse, as illustrated in Fig. 1(d). This is in contrast to appended CPMG acquisition, shown in Fig. 1(c), which requires any phase modulated coherence of order p_{in} to be converted into amplitude modulation via a z -filter before conversion into observable coherence of $p = -1$. Since PIETA avoids the need for a z -filter it gives a $\sqrt{2}$ improvement in sensitivity over CPMG acquisition and can also separate degenerate pathways that CPMG acquisition cannot.

While this use of a concerted phase increment is similar to “cogwheel,” the PIETA approach does not require a detailed analysis of the undesired pathways and the derivation of a master equation for the receiver phase. In fact, a PIETA spectrum can illustrate why no single master equation in conventional or “cogwheel” phase cycling will work for some

experiments. This is seen when combining PIETA with the 2D MQ-MAS experiment.²¹ Shown in Fig. 2(c) is the PIETA cross section for the two pulse MQ-MAS experiment²² combined with PIETA. In this experiment the phase modulated input coherence before mixing is $p_{in} = -3$. The acquisition of both pathway and anti-pathway signals for hypercomplex acquisition in t_1 results in a doubled PIETA pattern. While reducing this 4D signal of $S(t_1, t_2, n, \Delta p)$ down to the 2D signal, $S(t_1, t_2)$, is straightforward, it is not immediately clear how one can derive a receiver master equation for coaddition of signals that can be implemented on existing commercial spectrometer hardware using available phase cycling schemes.

Finally, PIETA can reduce errors in measuring transverse relaxation rates and J -couplings. Additionally, it can provide this information in a “pseudo-single-scan” experiment. “Single-scan” in the sense that the entire multi-dimensional time domain signal is acquired in a single acquisition, and “pseudo” because the separate “single-scan” signals must also be acquired along an excitation phase dimension. Sampling in the excitation phase dimension, however, need not increase the total experiment time since it is performed in lieu of conventional phase cycling and signal averaging.

This approach is illustrated with the 2D J PIETA ^1H spectrum for ethylbenzene in Fig. 3(a) and its 1D cross sections in Fig. 3(b). The multiplet structures and intensities are as expected and in good agreement with the simulated 2D cross sections for ethylbenzene shown in Fig. 3(d). In contrast, the 1D cross sections obtained from a 2D J CPMG ^1H spectrum, shown in Fig. 3(c), exhibit sharp zero frequency artifacts. Even in the presence of pulse imperfections, the echo decays measured with PIETA exhibit a mono-exponential decay while CPMG echoes exhibit a multi-exponential decay.¹¹

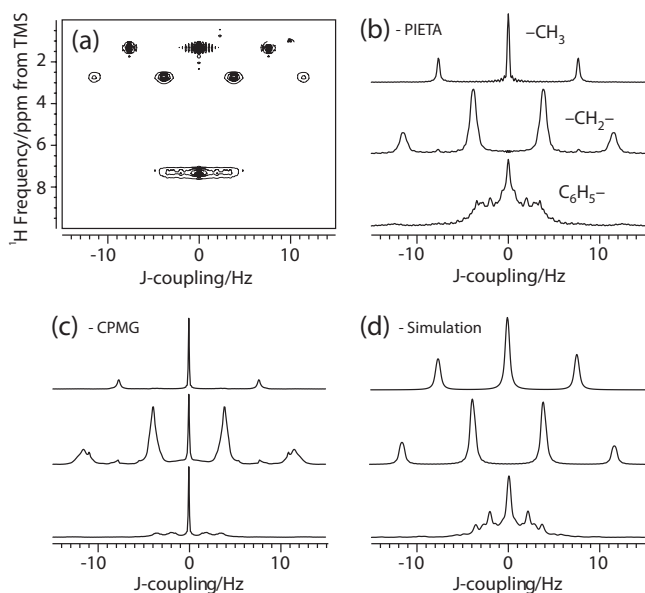


FIG. 3. (a) The 2D ^1H J spectrum of 10% ethylbenzene dissolved in CDCl_3 using PIETA using $\Delta\phi_P = 2\pi/128$. Comparison of 2D cross sections from (b) 2D J PIETA and (c) 2D J CPMG. In both the CPMG and PIETA cross sections there are small intensity sinc function artifacts related to the truncation of signal inside the constant time acquisition between the π pulses. The simulated 2D cross sections for ethylbenzene shown in (d). Simulation parameters and details are given in the supplementary material.¹⁹

Thus, PIETA is more robust with regards to rf pulse imperfections than CPMG in measuring transverse relaxation rates and J -couplings. Although the echo decay in PIETA is mono-exponential, it is still vulnerable to pulse imperfections, and the observed decay arises from both T_2 processes and cumulative coherence transfer inefficiencies.

In summary, PIETA can replace CPMG in every instance with little increase in experiment time, some additional signal processing steps, and significantly reduced artifacts. Additionally, unlike CPMG, PIETA can be appended to multi-dimensional NMR experiments with signals phase modulated from indirect evolution periods. Finally, PIETA opens the door to greater opportunities for the use of echo train acquisition in “pseudo-single-scan” 2D NMR spectroscopy. We believe this new approach will prove useful in numerous applications such as solution-state NMR of biological molecules,⁵ solid-state NMR J spectroscopy in non-crystalline solids,²³ improved MRI contrast,⁶ and mobile single-sided type NMR applications^{13,24} such as oil-well logging.²⁵

This material is based upon work supported by the National Science Foundation (NSF) under Grant No. NSF CHE-1012175.

¹P. Mansfield, “Multi-planar image formation using NMR spin echoes,” *J. Phys. C* **10**, L55–L58 (1977).

²H. Y. Carr and E. M. Purcell, “Effects of diffusion on free precession in nuclear magnetic resonance experiments,” *Phys. Rev.* **94**, 630–638 (1954).

³S. Meiboom and D. Gill, “Modified spin-echo method for measuring nuclear relaxation times,” *Rev. Sci. Instrum.* **29**, 688 (1958).

⁴G. Gaelman and M. G. Prammer, “The CPMG pulse sequence in strong magnetic field gradients with applications to oil-well logging,” *J. Magn. Reson., Ser. A* **113**, 11–18 (1995).

⁵A. Ross, M. Czisch, and G. C. King, “Systematic errors associated with the CPMG pulse sequence and their effects on motional analysis of biomolecules,” *J. Magn. Reson., Ser. A* **124**, 355–365 (1997).

⁶W. Foltz, J. Stainsby, and G. Wright, “ T_2 accuracy on a whole-body imager,” *Magn. Reson. Med.* **38**, 759–768 (1997).

⁷L. Frydman, T. Scherf, and A. Lupulescu, “The acquisition of multidimensional nmr spectra within a single scan,” *Proc. Natl. Acad. Sci. U.S.A.* **99**, 15858–15862 (2002).

⁸N. M. Szeverenyi, A. Bax, and G. E. Maciel, “Magic-angle hopping as an alternative to magic-angle spinning for solid-state NMR,” *J. Magn. Reson., Ser. A* **61**, 440 (1984).

⁹P. J. Grandinetti, J. T. Ash, and N. M. Trease, “Symmetry pathways in solid-state NMR,” *Prog. Nucl. Magn. Reson. Spectrosc.* **59**, 121–196 (2011).

¹⁰R. Freeman and H. D. W. Hill, “High-resolution study of nmr spin echoes: “ J spectra,”” *J. Chem. Phys.* **54**, 301–313 (1971).

¹¹R. L. Vold, R. R. Vold, and H. E. Simon, “Errors in measurements of transverse relaxation rates,” *J. Magn. Reson.* **11**, 283–298 (1973).

¹²G. Gaelman and M. G. Prammer, “Analysis of Carr-Purcell sequences with nonideal pulses,” *J. Magn. Reson. B* **109**, 301–309 (1995).

¹³F. Bălibanu, K. Hailu, R. Eymael, D. Demco, and B. Blümich, “Nuclear magnetic resonance in inhomogeneous magnetic fields,” *J. Magn. Reson.* **145**, 246–258 (2000).

¹⁴Y.-Q. Song, “Categories of coherence pathways for the CPMG sequence,” *J. Magn. Reson.* **157**, 82–91 (2002).

¹⁵A. D. Bain, “Coherence levels and coherence pathways in NMR. A simple way to design phase cycling procedures,” *J. Magn. Reson.* **56**, 418–427 (1984).

¹⁶G. Bodenhausen, H. Kogler, and R. R. Ernst, “Selection of coherence-transfer pathways in NMR pulse experiments,” *J. Magn. Reson.* **58**, 370–388 (1984).

¹⁷M. H. Levitt, P. K. Madhu, and C. E. Hughes, “Cogwheel phase cycling,” *J. Magn. Reson.* **155**, 300–306 (2002).

¹⁸G. Drobny, A. Pines, S. Sinton, D. Weitekamp, and D. Wemmer, “Fourier transform multiple quantum nuclear magnetic resonance,” *Faraday Symp. Chem. Soc.* **13**, 49–55 (1978).

- ¹⁹See supplementary material at <http://dx.doi.org/10.1063/1.4728105> for phase cycling theory review, PIETA signal processing, and J coupling simulation details.
- ²⁰K. Dey, J. T. Ash, N. M. Trease, and P. J. Grandinetti, "Trading sensitivity for information: CPMG acquisition in solids," *J. Chem. Phys.* **133**, 054501 (2010).
- ²¹L. Frydman and J. S. Harwood, "Isotropic spectra of half-integer quadrupolar spins from bidimensional magic-angle spinning NMR," *J. Am. Chem. Soc.* **117**, 5367–5369 (1995).
- ²²D. Massiot, B. Touzo, D. Trumeau, J. P. Coutures, J. Virlet, P. Florian, and P. J. Grandinetti, "Two-dimensional magic-angle spinning isotropic reconstruction sequences for quadrupolar nuclei," *Solid State Nucl. Magn. Reson.* **6**, 73–83 (1996).
- ²³P. Florian, F. Fayon, and D. Massiot, "²⁹Si–O–Si scalar spin-spin coupling in the solid state: Crystalline and glassy wollastonite CaSiO₃," *J. Phys. Chem. C* **113**, 2562–2572 (2009).
- ²⁴B. Blümich, J. Perlo, and F. Casanova, "Mobile single-sided NMR," *Prog. Nucl. Magn. Reson. Spectrosc.* **52**, 197–269 (2008).
- ²⁵Y.-Q. Song, H. Cho, T. Hopper, A. E. Pomerantz, and P. Z. Sun, "Magnetic resonance in porous media: Recent progress," *J. Chem. Phys.* **128**, 052212 (2008).

Phase Incremented Echo Train Acquisition in NMR Spectroscopy

Jay H. Baltisberger,¹ Brennan J. Walder,² Eric G. Keeler,² Derrick C. Kaseman,² Kevin J. Sanders,² and Philip J. Grandinetti²

¹*Division of Natural Science, Mathematics, and Nursing, Berea College, Berea, Kentucky 40403*

²*Department of Chemistry, Ohio State University, 100 West 18th Avenue, Columbus, OH 43210, USA^{a)}*

(Dated: 1 May 2012)

I. REVIEW OF PHASE CYCLING AND THE MASTER EQUATION

In an NMR experiment with M phase cycled excitation pulses or excitation pulse blocks, the excitation phases are represented in a vector with M elements,

$$\phi = (\phi_1, \phi_2, \dots, \phi_M). \quad (1)$$

The Fourier transform of the *excitation phase domain signal* as a function of the M excitation phases yields a M -dimensional *pathway difference domain spectrum*¹,

$$\mathbf{s}(\Delta\mathbf{p}) = \int_0^{2\pi} d\phi_1 \int_0^{2\pi} d\phi_2 \cdots \int_0^{2\pi} d\phi_M \mathbf{s}(\phi) e^{i\Delta\mathbf{p} \cdot \phi}, \quad (2)$$

where $\Delta\mathbf{p}$ is a coherence transfer pathway difference vector, with M elements,

$$\Delta\mathbf{p} = (\Delta p_1, \Delta p_2, \dots, \Delta p_M), \quad (3)$$

each given by $\Delta p_m = p_m - p_{m-1}$. This pathway difference vector can be derived from the coherence transfer pathway vector, with $M + 1$ elements,

$$\mathbf{p} = (p_0, p_1, \dots, p_M), \quad (4)$$

with $p_0 = 0$ and $p_M = -1$. The pathway difference domain spectrum is a line spectrum. It can be visualized as an M -dimensional hypermatrix containing the pathway difference resonance lines for all excited transitions. The elements of this hypermatrix are indexed by a $\Delta\mathbf{p}$ vector. The range of Δp indexes is dependent on the spin systems within the sample. Generally, a single spin I will have coherence orders extending over $-2I \leq p \leq 2I$. More generally, N coupled spins will have coherence orders extending over $-2L \leq p \leq 2L$, where $L = \sum_k I_k$. Thus, the integer range of Δp values is from $-4L$ to $+4L$. Assuming the NMR experiment begins with the system in some form of longitudinal order, such as Zeeman order, with a coherence order of $p_0 = 0$, then the integer range of Δp_1 values is from $-2L$ to $+2L$. Similarly, if we assume that the NMR experiment ends with

perfect quadrature detection of transverse magnetization with $p_M = -1$, then the integer range of Δp_M values is from $-2L - 1$ to $+2L - 1$. In modern spectrometers with digital quadrature detection this is a good assumption. In spectrometers with analog quadrature detection, however, there can be imperfections which lead to the detection of transverse magnetization with $p_M = +1$. Then, the integer range of Δp_M values also includes values from $-2L + 1$ to $+2L + 1$, making the total range Δp_M values from $-2L - 1$ to $+2L + 1$.

While the phase increments needed to sample the signal in the ϕ space comes from the Nyquist-Shannon theorem², it is only necessary to choose phase increments that do not alias undesired pathway signals onto the desired pathway signals.

Although the idea of a Fourier transform with respect to pulse phase was first demonstrated¹ in the late 1970's, computer hardware limitations prevented it from being used as a real time approach in pulsed NMR spectroscopy. The most popular “work around” for this problem has been to cycle the receiver phase according to a “master equation” to take projections in the ϕ space which correspond to a (zero dimensional) cross section containing the desired pathway signal in the $\Delta\mathbf{p}$ space^{3,4}.

This approach can be visualized by shifting the desired pathway resonance, $\Delta\mathbf{p}$, to the origin of the M -dimensional pathway difference spectrum,

$$\mathbf{s}'(\Delta\mathbf{p}') = \mathbf{s}(\Delta\mathbf{p} - \Delta\mathbf{p}) \quad (5)$$

using the Fourier shift theorem,

$$\mathbf{s}(\Delta\mathbf{p} - \Delta\mathbf{p}) \leftrightarrow e^{-i\phi \cdot \Delta\mathbf{p}} \cdot \mathbf{s}(\phi), \quad (6)$$

to obtain a transformed excitation phase domain signal,

$$\mathbf{s}'(\phi') = e^{-i\phi \cdot \Delta\mathbf{p}} \cdot \mathbf{s}(\phi). \quad (7)$$

From the Fourier relationship between excitation phase and pathway difference domains¹, the desired pathway can be obtained through integration of this transformed excitation phase domain signal,

$$\mathbf{s}'(\mathbf{0}) = \int_0^{2\pi} d\phi'_1 \int_0^{2\pi} d\phi'_2 \cdots \int_0^{2\pi} d\phi'_M \mathbf{s}'(\phi'). \quad (8)$$

This approach is combined with signal averaging, with the “master equation” for the receiver phase implementing the Fourier shift,

$$\phi_{\text{rcvr}} = -\phi \cdot \Delta\mathbf{p}, \quad (9)$$

^{a)}<http://www.grandinetti.org>

as signals are acquired at different excitation phases to calculate the integral given by

$$\mathbf{s}'(\mathbf{0}) = \int_0^{2\pi} d\phi_1 \int_0^{2\pi} d\phi_2 \cdots \int_0^{2\pi} d\phi_M [e^{i\phi_{\text{rcvr}}} \cdot \mathbf{s}(\phi)]. \quad (10)$$

The conventional approach for calculating this integral is to perform “nested” phase cycling. When implemented on an NMR spectrometer, the integrals are approximated as summations, and the desired signal is given by

$$\mathbf{s}'(\mathbf{0}) = \sum_{\phi_1=0}^{\phi_1 < 2\pi} \Delta\phi_1 \sum_{\phi_2=0}^{\phi_2 < 2\pi} \Delta\phi_2 \cdots \sum_{\phi_M=0}^{\phi_M < 2\pi} \Delta\phi_M [e^{i\phi_{\text{rcvr}}} \cdot \mathbf{s}(\phi)]. \quad (11)$$

To avoid aliasing of undesired pathway difference resonances onto the desired pathway difference resonance, the $\Delta\phi_i$ values are typically set to

$$\Delta\phi_i = \frac{2\pi}{N_i}, \quad (12)$$

where

$$N_i = \Delta p_{i,\text{max}} - \Delta p_{i,\text{min}} + 1. \quad (13)$$

This approach, however, is overkill, since many elements in the pathway difference hypermatrix will be zero; that is, some $\Delta\mathbf{p}$ resonances have no intensity. Additionally, there is no need to prevent aliasing among the undesired pathway difference resonances. Thus, with insight about the pathway difference spectrum the value N_i can often be significantly reduced. Cogwheel phase cycling attempts to find a canonical transformation of ϕ space down to a single phase, eliminating the need for nested phase cycling.

The challenge with traditional phase cycling as well as cogwheel phase cycling approach, however, is what to do when there are multiple desired pathway signals, $\Delta\mathbf{P}^{(j)}$. Since there is only one receiver phase, a solution to the simultaneous master equations,

$$\phi_{\text{rcvr}} = -\phi \cdot \Delta\mathbf{P}^{(j)}, \quad (14)$$

may not exist. There have been some “conjectures” about possible solutions using cogwheel phase cycling⁵, but, in general, no algorithm for finding the canonical cogwheel transformation and solution exists.

Consider, for example, the experimental 2D PIETA cross section from a 3D MAS-PIETA spectrum of $^{87}\text{RbNO}_3$ shown in Fig. 2 of the main text. Here, each echo contains one desired pathway signal, whose value of ΔP varies with echo count, n . One can derive the master equations for the receiver as a function of echo count, given by

$$\phi_{\text{rcvr}}(n) = -\phi_P \Delta P(n), \quad (15)$$

where

$$\Delta P(n) = \begin{cases} 2 \left\lfloor \frac{n-1}{2} \right\rfloor + 2 & \text{for even } n, \\ -2 \left\lfloor \frac{n-1}{2} \right\rfloor - 2 & \text{for odd } n, \end{cases} \quad (16)$$

where $\lfloor x \rfloor$ represents the integer part or floor function of x . While implementation of this echo count dependent receiver phase should be relatively straightforward on modern NMR spectrometers, unfortunately, for many working spectrometers this is not possible.

Next consider the experimental 2D PIETA cross section in Fig. 3 from a 4D MQ-MAS-PIETA spectrum of $^{87}\text{RbNO}_3$ obtained with the pulse sequence shown in Fig. S1. Here, each echo contains two desired pathway signals, whose values of ΔP vary with echo count, n , according to

$$\Delta P(n) = \begin{cases} 2 \left\lfloor \frac{n-1}{2} \right\rfloor + 4 & \text{for even } n, \\ 2 \left\lfloor \frac{n-1}{2} \right\rfloor - 2 & \text{for even } n, \\ -2 \left\lfloor \frac{n-1}{2} \right\rfloor + 2 & \text{for odd } n, \\ -2 \left\lfloor \frac{n-1}{2} \right\rfloor - 4 & \text{for odd } n. \end{cases} \quad (17)$$

While it may be possible to define a single master equation for the receiver phase as a function of echo count which aliased the two desired pathway signals together without undesired pathways, the algorithm for implementing such a scheme on a commercial spectrometer would be challenging at best, or perhaps even impossible.

A much simpler, and obvious solution, utilized in PIETA, is to abandon the “work around” solution of using the receiver phase to take the projections in ϕ space. We no longer have the computer hardware limitations of the 1980’s, and can easily afford to elevate sampling in ϕ space to the same status as sampling in t space. While this increases the dimensionality of NMR signals, it adds no additional time to the length of an experiment already implemented using conventional or cogwheel phase cycling.

II. PIETA SIGNAL PROCESSING

Generally, when PIETA is appended to a N -dimensional NMR experiment, the signal acquired has $N + 2$ dimensions, with the additional two dimensions associated with the excitation phase and the echo count (n). The $N + 2$ dimensional signal can be reduced back to $N + 1$ dimensions by: (1) applying a Fourier transform of the signal with respect to the excitation phase dimension to obtain the signal as a function of the Δp dimension, and (2) extracting cross-sections through the Δp and echo count (n) dimensions using the desired pathway equations, such as Eq. (16) or (17). This yields a $N+1$ -dimensional NMR signal that includes an echo count dimension (n) or an evolution time that is an

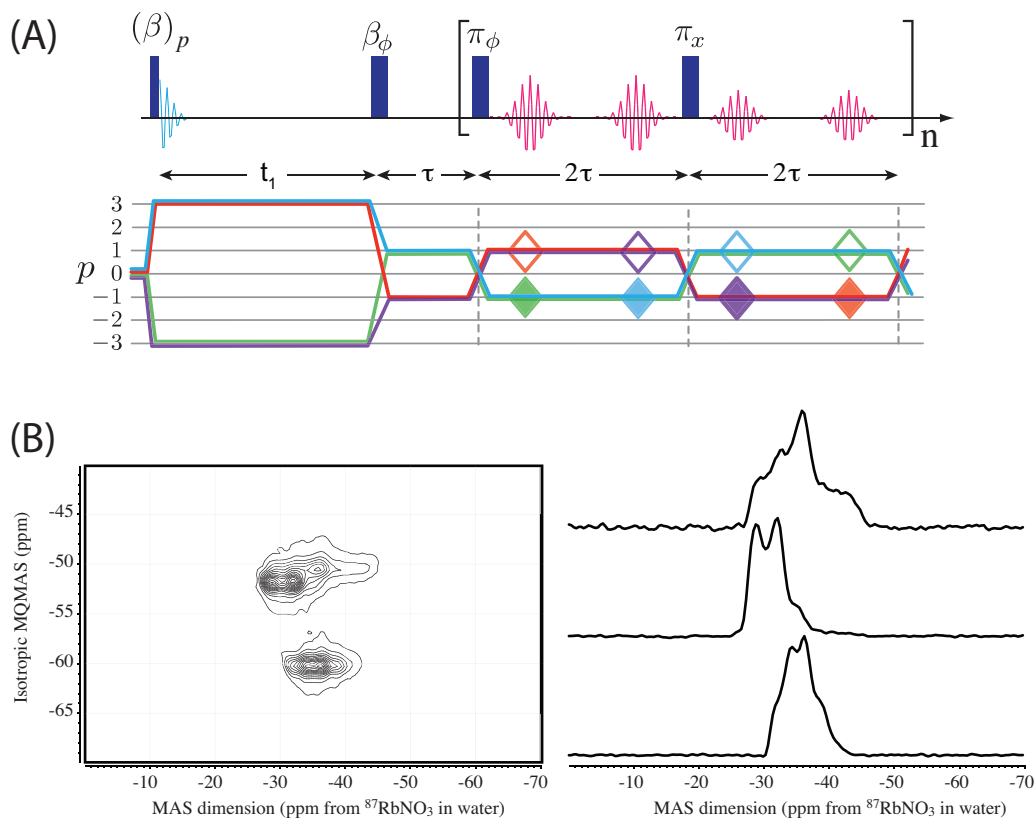


FIG. 1. (A) The MQ-MAS-PIETA pulse sequence. (B) 2D MQ-MAS spectrum of RbNO_3 along with cross-sections for the three sites obtained after processing. This spectrum was obtained by co-adding the 2D MQ-MAS spectrum for the 4 pathways in Eq. (17) with appropriate weighting to optimize sensitivity.

integer multiple of the spacing between echo maxima. If the echoes are modulated by J couplings, then a Fourier transform of the signal along this dimension yields the J spectrum. If there is no modulation along the echo count dimension then a sensitivity enhancement can be obtained by projecting out the dimension after applying a apodization with a matched filter to optimize sensitivity⁶. The resulting signal can then be processed as one would have without PIETA.

III. SIMULATION OF ETHYLBENZENE IN FIG. 3

The ^1H J -couplings in ethylbenzene were determined in a least-squares analysis of the ^1H spectrum of the phenyl region for ethylbenzene. The spectrum was modeled using a full diagonalization of the 5 spin Hamiltonian. The best fit values are given in Table I. The resulting parameters were then used in SIMPSON⁷ to simulate the C_6H_5 region of the J -resolved PIETA. Our

model ignores any weak long range coupling with the CH_2 , which would explain the additional experimental broadening not seen in the simulation.

- ¹G. Drobny, A. Pines, S. Sinton, D.P. Weitekamp, and D. Wemmer. Fourier transform multiple quantum nuclear magnetic resonance. *Symp. Faraday Soc.*, 13:93, 1980.
- ²C. E. Shannon. Communication in the presence of noise. *Proc. Institute of Radio Engineers.*, 37:10–12, 1949.
- ³G. Bodenhausen, H. Kogler, and R. R. Ernst. Selection of coherence-transfer pathways in NMR pulse experiments. *J. Magn. Reson.*, 58:370–388, 1984.
- ⁴A. D. Bain. Coherence levels and coherence pathways in NMR. a simple way to design phase cycling procedures. *J. Magn. Reson.*, 56:418–427, 1984.
- ⁵C. E. Hughes, M. Carravetta, and M. H. Levitt. Some conjectures for cogwheel phase cycling. *J. Magn. Reson.*, 167:259–265, 2004.
- ⁶K.K. Dey, J. T. Ash, N. M. Trease, and P. J. Grandinetti. Trading sensitivity for information: CPMG acquisition in solids. *J. Chem. Phys.*, 133:05401–01–054501–10, 2010.
- ⁷M. Baks, J. T. Rasmussen, and N. Chr. Nielsen. SIMPSON: A general simulation program for solid-state NMR spectroscopy. *J. Magn. Reson.*, 147:296–330, 2000.

site	chem. shift/ppm	1	2	3	4	5
1	-10.6	-	7.75 Hz	1.78 Hz	0.77 Hz	1.47 Hz
2	16.6	-	-	7.20 Hz	1.85 Hz	0.77 Hz
3	-14.6	-	-	-	7.20 Hz	1.77 Hz
4	16.6	-	-	-	-	7.75 Hz
5	-10.6	-	-	-	-	-

TABLE I. Chemical shift and J coupling parameters used in the ^1H J spectrum simulation of ethylbenzene.